

## Article

# Production and Characterization of Wild Sugarcane (*Saccharum spontaneum* L.) Biochar for Atrazine Adsorption in Aqueous Media

Josué Prens<sup>1,2</sup>, Zohre Kurt<sup>3,4</sup>, Arthur M. James Rivas<sup>2,5,\*</sup>  and Jorge Chen<sup>2,5</sup>

<sup>1</sup> Department of Hydraulics, Sanitary, and Environmental Sciences, Universidad Tecnológica de Panamá, Panama City 0819-07289, Panama

<sup>2</sup> Research Group—Iniciativa de Integración de Tecnologías para el Desarrollo de Soluciones Ingenieriles (I2TEDSI), Universidad Tecnológica de Panamá, Panama City 0819-07289, Panama

<sup>3</sup> Department of Environmental Engineering, Middle East Technical University, 06800 Ankara, Turkey

<sup>4</sup> Chemistry Department, Republic of Panama Campus, Florida State University, Panama City 0843-03081, Panama

<sup>5</sup> Department of Mechanical Engineering, Universidad Tecnológica de Panamá, Panama City 0819-07289, Panama

\* Correspondence: arthur.james@utp.ac.pa

**Abstract:** Wild sugarcane (*Saccharum spontaneum* L.) is an invasive plant species in the Central American region. Due to its low nutrient and water requirements, it can grow fast and displace native species. Therefore, its biomass is considered a waste to prevent the further distribution of the specie. This study investigates the production and characterization of wild sugarcane biochar to provide a use for its waste. The produced biochar was used for atrazine adsorption in aqueous solutions to provide a possible application of this biochar near the water bodies that were often detected to be contaminated with atrazine. The biochar was produced via top-lit updraft gasification with airflow rates between 8 to 20 L/min, achieving yields ranging from 22.9 to 27.5%. Batch experiments revealed that biochar made at 12 L/min presented the best removal efficiency (37.71–100%) and the maximum adsorption capacity ( $q_m = 0.42$  mg/g). Langmuir ( $R^2 = 0.94$ – $0.96$ ) and Freundlich ( $R^2 = 0.89$ – $0.97$ ) described the experimental data appropriately. Fourier transform infrared spectroscopy suggested that atrazine removal in wild sugarcane biochar could be mainly due to carboxylic functional groups. In addition, the biochar organic carbon composition contributed to a higher removal capacity in biochar produced at different airflow rates.

**Keywords:** *Saccharum spontaneum*; atrazine; top-lit updraft; gasifier; biochar



**Citation:** Prens, J.; Kurt, Z.; James Rivas, A.M.; Chen, J. Production and Characterization of Wild Sugarcane (*Saccharum spontaneum* L.) Biochar for Atrazine Adsorption in Aqueous Media. *Agronomy* **2023**, *13*, 27. <https://doi.org/10.3390/agronomy13010027>

Academic Editors: Xiaoyun Xu and Fan Yang

Received: 16 November 2022

Revised: 17 December 2022

Accepted: 20 December 2022

Published: 22 December 2022



**Copyright:** © 2022 by the authors. Licensee MDPI, Basel, Switzerland. This article is an open access article distributed under the terms and conditions of the Creative Commons Attribution (CC BY) license (<https://creativecommons.org/licenses/by/4.0/>).

## 1. Introduction

Invasive plants disrupt natural habitats by displacing native species and disturbing nutrient cycling [1]. On the other hand, most of these species possess strong adaptability and quick reproduction capacities. In addition, invasive grasses species promote fires during dry seasons [2]. Invasive plant species include perennial grasses and trees [3,4]. However, these plants can be troublesome, often leading to high removal costs. Therefore, various methods have been developed to control and remove invasive plants, including mechanical methods and herbicides [1]. Wild sugarcane (*Saccharum spontaneum* L.) is an invasive plant species in Central America and has been naturalized in some countries, such as France, Costa Rica, and Panama [3]. It is a lignocellulosic, C4-type plant capable of reproducing from layering, vegetative growth, and seeding [2,5]. It is a highly polymorphous plant ( $2n = 40$ – $128$ ), growing from a few centimeters to six meters tall. Wild sugarcane has been used in controlled conditions for phytoremediation, CO<sub>2</sub> sequestration, and the denitrification of drinking water [6–9]. However, due to its fast growth with little nutrient input, it can endanger native plant species. The Panama Canal spends between \$550/ha and \$2570/ha annually to control the spread of wild sugarcane in the watershed due to its fast growth that displaces native plant species [10].

Wild sugarcane covers approximately 6932 ha of the Panama Canal watershed, representing a growing ecosystem problem. However, the available biomass produced by this plant could be a potential biomass source for biofuel and biomaterial production [11] that could further be used to remediate contaminated soils and waters.

Atrazine (2-chloro-4-[ethylamino]-6-[isopropylamino]-s-triazine) is a synthetic herbicide from the triazine family. It is used in corn, sugarcane, and sorghum crops to control grasses and broadleaf weeds [12,13]. Despite being banned in the European Union (EU), atrazine is still the second most-used herbicide worldwide [12,14]. Atrazine is highly toxic and has high water mobility, remarkable chemical stability, and a long half-life in soils (41–231 days). Hence, atrazine threatens non-target plants, animals, and humans [14,15]. In addition, atrazine has been reported to increase cancer risk, disrupt endocrine production, and cause human feminization [12,14–16]. Many soils and water bodies in Central America have been reported to be contaminated with atrazine. Chemical, microbial, and photocatalytic degradation are methods implemented to remove this herbicide from water and soils [12]. However, the degradation processes of this contaminant are often expensive and too complicated. Therefore, low-cost methods to remove this contaminant are necessary [15].

Biochar is a carbonaceous material made from the thermochemical decomposition of biomass. It can be produced via pyrolysis or gasification, providing a simple way to be used in different applications. Biochar has proved an excellent asset for soil amendment and crop yield increase [17–19]. Moreover, biochar can be applied to aqueous solutions for organic and inorganic pollutant removal [20]. Unmodified biochar has shown evidence of good atrazine removal capacity [21]. Additionally, it has been reported that atrazine removal can be further increased with biochar enhanced by additives [15,22]. However, no studies have been performed to explore the potential to use an invasive-species-based biochar to remove atrazine from aqueous solutions.

This study aimed to produce and characterize biochar from wild sugarcane waste for simplified atrazine removal in aqueous media. Atrazine adsorption experiments were carried out to evaluate wild sugarcane biochar performance.

## 2. Materials and Methods

### 2.1. Biochar Production

Wild sugarcane samples were collected from an empty grassland in north Panama. The location was selected based on Aguilar et al.'s [11] methodology. After gathering, wild sugarcane samples were dried at room temperature until the moisture content was below 10%. Later, the samples were milled and sieved between 2.00–4.75 mm particle sizes. A top-lit updraft gasifier (TLUD) was used to produce biochar based on James et al. design [23]. Figure 1 shows a schematic diagram of biochar production in a TLUD gasifier. Three type-k thermocouples (TC-1, TC-2, and TC-3) were connected to a data logger and were used to monitor the flame position during the carbonization process. In addition, air was used as the gasification agent, and four airflows (8, 12, 16, and 20 L/min) were evaluated. This work identifies biochar as BCX, with the X representing the gasification airflow rate (e.g., BC8). After the process, the TLUD gasifier was allowed to cool down to room temperature before biochar extraction.

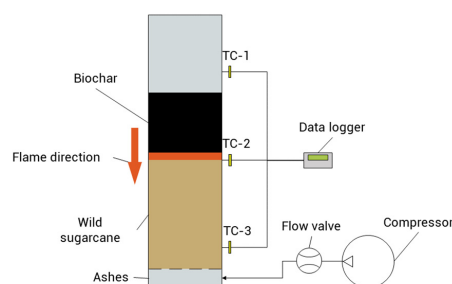


**Figure 1.** Schematic diagram of wild sugarcane biochar production in a top-lit updraft gasifier. TC-1, TC2, and TC-3 represent the 3 thermocouples connected to the data logger.

## 2.2. Biochar Characterization

Proximate analysis was performed on the wild sugarcane raw material and biochar, following James et al.'s methodology and ASTM standards D3173-97 [24], D3175-89 (02) [25], and D3172-89 (02) [23,26]. Two grams of biochar were heated up to 100 °C, 500 °C, and 900 °C to determine mass loss due to the release of moisture content, volatile matter, and fixed carbon, respectively. Ash content was determined by differences. *S. spontaneum* values for moisture content, volatile matter, fixed carbon, and ash are presented in Table 1. The pH analysis was described in a previous study [27] according to the standard methods procedure [28]. Twenty grams of biochar was mixed with de-ionized water for 2 h. The resulting solution was filtered two times, first with filter #1240 and later with filter #1242, both Filter-Lab® (Barcelona, Spain). The pH level was measured with a pH meter (ThermoScientific®, ORION VERSATAR PRO™, Waltham, MA, USA). Total N was determined using the AOAC Official Method 993.13. In addition, total P<sub>2</sub>O<sub>5</sub>, K<sub>2</sub>O, Mg, CaO, and Zn were determined using the AOAC Official Methods 958.01, 958.02, 984.01, 945.04, and 975.02, respectively [29]. Organic carbon (O.C.) was analyzed using the Walkley–Black method [30]. For all analyses, 20 mg of biochar was used.

**Table 1.** *Saccharum spontaneum* L. feedstock proximate analysis.

Parameter	Unit	Value
Moisture	%	9.47 ± 1.54
Volatile matter	%	80.49 ± 1.49
Fixed carbon	%	4.72 ± 1.62
Ash	%	5.32 ± 3.17

Biochar surface area was measured with the Brunauer–Emmett–Teller (BET) method, as stated by James et al. [31]. A total of 0.4 g of biochar was collected for nitrogen adsorption at −196 °C, with previous degassing at 110 °C and 1 mmHg. A Fourier transform infrared (FTIR) spectroscopy analysis was carried out for wild sugarcane feedstock and biochars to determine the surface functional groups. The samples were crushed and mixed with KBr to generate the curves. A thermogravimetric analysis (TGA) was performed to determine the thermal degradation of wild sugarcane feedstock (WSF). A total of 10 mg of WSF was pyrolyzed at 5, 10, 15, and 20 °C/min in a nitrogen atmosphere, with a 100 mL/min flow. The temperature range was from 30 °C to 800 °C.

## 2.3. Adsorption Experiments

Atrazine stock solution was prepared by mixing atrazine and water. First, atrazine concentrations of 0.5 and 30 mg/L were prepared to evaluate the biochars' adsorption capacities. Then, 0.3 g of biochar was sieved through a 250–600 µm mesh, and 10 mL of the solution was prepared with the desired atrazine concentrations. The final atrazine solution used in experiments contained 0.01 M CaCl<sub>2</sub> to keep the ionic strength constant and 200 mg/L sodium azide (NaN<sub>3</sub>) to eliminate the biological activity. The solution pH varied between 6.3 and 6.7. The atrazine–biochar mixtures were stirred at 200 rpm for 48 h and kept at 25 °C. Supernatants of the samples were taken with triplicates from each tube. Then, samples were centrifuged at 10,000 × g for 15 min before injected into the high-performance liquid chromatograph (HPLC). The experimental values of q<sub>e</sub> (mg/g) and the adsorption efficiency E (%) were calculated (1) and (2).

$$q_e = ((C_0 - C_e) \times V)/m, \quad (1)$$

$$E = ((C_0 - C_e)/C_e) \times 100, \quad (2)$$

C<sub>0</sub> is the initial concentration (mg/L); C<sub>e</sub> (mg/L) represents the concentration of atrazine at equilibrium; V is the volume of the solution (L), and m is the mass of biochar (g). Langmuir (3) and Freundlich (4) isotherms were used for fitting the isotherm data.

$$q_{eq} = (q_m \times K_L \times C_e)/(1 + K_L \times C_e), \quad (3)$$

$$q_{eq} = K_F \times (C_e)^{(1/n)}, \quad (4)$$

where  $q_{eq}$  represents the adsorption amount in equilibrium (mg/g);  $q_m$  is the maximum adsorption amount (mg/g);  $K_L$  (L/mg) and  $K_F$  ((mg/g)  $\times$  (L/mg)<sup>1/n</sup>) are the Langmuir and Freundlich constants, respectively, and the parameter  $n$  is the Freundlich index related to adsorption strength.

#### 2.4. Statistical Analysis

Analyses were conducted in triplicate, except for the TGA, N, P, K, Ca, Mg, and Zn, which were run in duplicate. Tukey's HSD test was performed to find significant differences between airflow rates, with an alpha ( $\alpha$ ) value of 0.05. The statistical analysis was accomplished using Microsoft<sup>®</sup> Excel<sup>®</sup> for Microsoft 365 MSO (Version 2209 Build 16.0.15629.20152) 64-bit.

### 3. Results

#### 3.1. Airflow Effect on Biochar Properties

The maximum gasification temperature was recorded as the flaming pyrolysis layer passed through the middle thermocouple (TC-2). The temperature showed a positive correlation with airflow rate ( $R^2 = 0.94$ ), while the maximum temperatures ranged from  $556.70 \pm 13.71$  °C to  $642.04 \pm 22.19$  °C, as shown in Figure 2a. In contrast, the yield of wild sugarcane biochar (WSB) decreased with increasing airflow rate (Figure 2b). BC8 exhibited the highest yield ( $27.59 \pm 0.94\%$ ), while BC20 showed the lowest yield ( $22.96 \pm 0.63\%$ ). Furthermore, the burning rate (BR) increased with airflow rates since more biomass was needed to reach higher temperatures. BC8 showed the lowest BR ( $8.53 \pm 0.47$  g/min) and BC20 (Figure 3a).

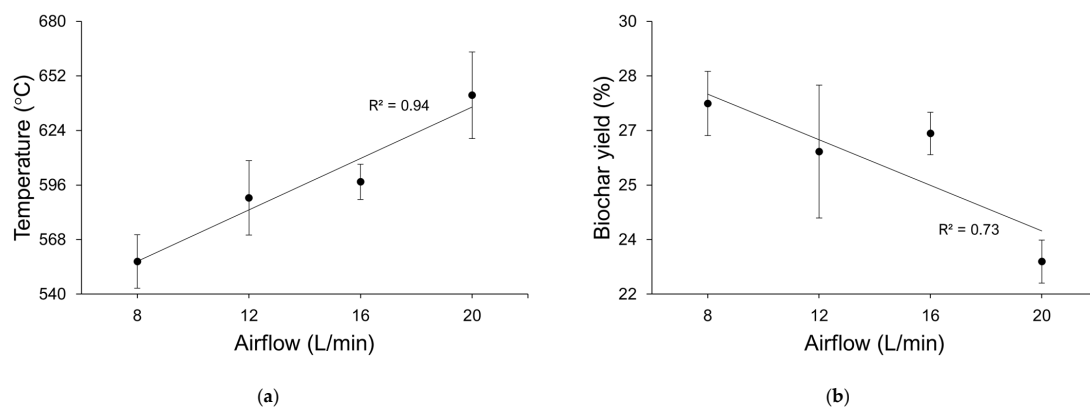


**Figure 2.** Airflow effect on: (a) gasification maximum temperatures; (b) wild sugarcane biochar yield.

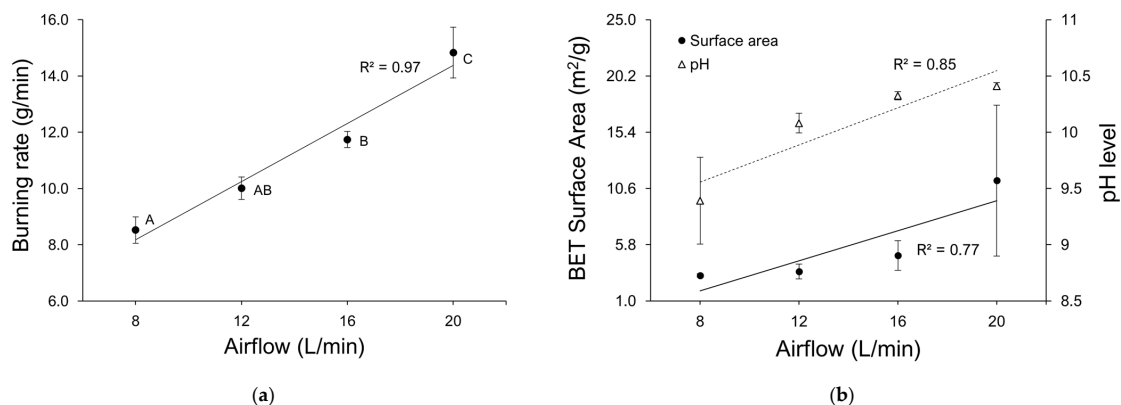


**Figure 3.** Airflow effect on: (a) gasification burning rate; (b) wild sugarcane biochar pH and BET surface area. Different letters indicate a significant difference.

Figure 3b presents the pH and BET surface area results of WSB. The produced biochar exhibited a pH higher than 9 in all cases. The pH levels increased with airflow, from  $9.39 \pm 0.77$  to  $10.41 \pm 0.07$  for BC8 and BC20, respectively. The pH increase with airflow ( $R^2 = 0.85$ ) is attributed to the higher reaction temperature and the degree of oxidation due to the carbonization process by the gasification of biomass [31]. The WSB surface area also increased as airflow rates were increased. BC8 ( $3.11 \pm 0.14 \text{ m}^2/\text{g}$ ) showed the lowest BET surface area, and BC20 ( $11.26 \pm 6.44 \text{ m}^2/\text{g}$ ) showed the highest. Figure 4 shows the results of  $\text{N}_2$  adsorption for BET analysis. BC20 exhibited the highest biochar  $\text{N}_2$  adsorption compared with other biochar. This could be due to the higher production temperature achieved during gasification that promoted higher biomass devolatilization [23].

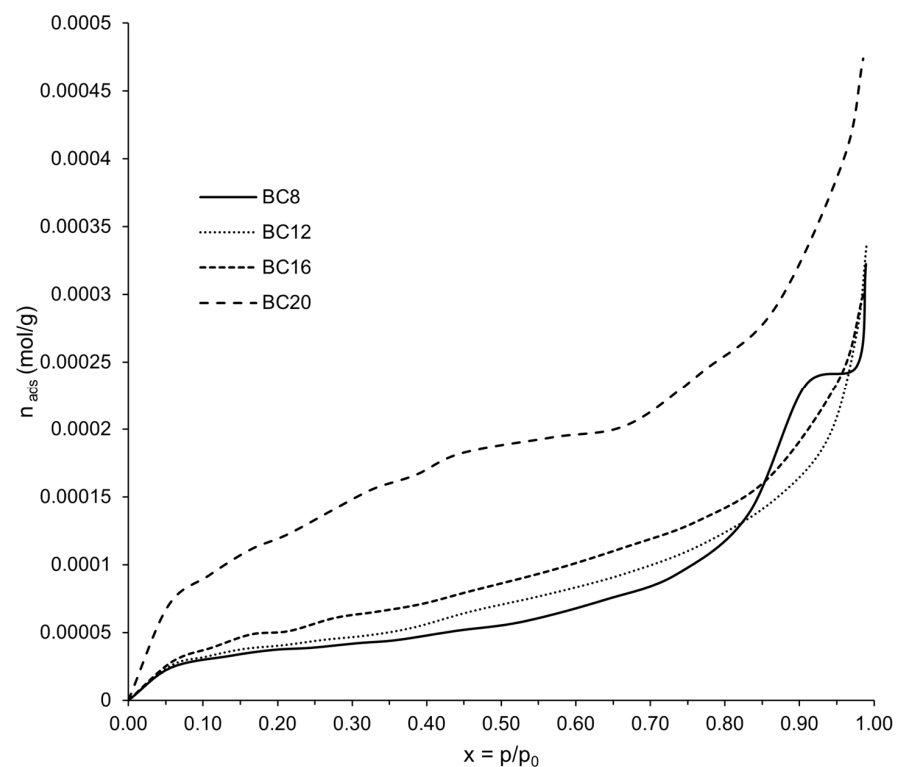


**Figure 4.** Nitrogen adsorption of wild sugarcane biochar (WSB) produced at different airflow rates. BC stands for biochar, and the number represents the airflow rate used for gasification, e.g., BC8—8 L/min.

Table 2 summarizes the results of proximate analysis on wild sugarcane biochar. Biomass carbonization reduced average wild sugarcane biochar moisture and volatile matter and increased fixed carbon and ash content compared with unreacted biomass. WSB moisture decreased with rising airflow rates, from  $7.09 \pm 1.85\%$  to  $3.49 \pm 0.85\%$ , for BC8 and BC16, respectively. The biochar moisture also showed an  $R^2$  correlation of 0.61 when the different airflow levels were compared. Fixed carbon and volatile matter showed no linear relation with airflow during the carbonization process.

**Table 2.** Airflow effect on wild sugarcane biochar proximate analysis.

Parameter	Unit	BC8	BC12	BC16	BC20	$R^2$
Moisture	%	$7.09 \pm 1.85^a$	$4.01 \pm 0.24^b$	$3.49 \pm 0.85^b$	$3.89 \pm 0.55^b$	0.61
Volatile matter	%	$42.85 \pm 7.64^a$	$42.77 \pm 4.23^a$	$42.18 \pm 10.91^a$	$43.82 \pm 13.07^a$	0.25
Fixed carbon	%	$30.96 \pm 3.76^a$	$33.25 \pm 3.44^a$	$32.78 \pm 9.48^a$	$27.24 \pm 9.71^a$	0.01
Ashes	%	$19.10 \pm 4.17^a$	$19.97 \pm 1.12^a$	$21.55 \pm 2.01^a$	$25.06 \pm 3.49^a$	0.81

BC8: biochar produced at 8 lpm; BC12: biochar produced at 12 lpm; BC16: biochar produced at 16 lpm; BC20: biochar produced at 20 lpm. Values followed by a different letter are significantly different at  $\alpha = 0.05$  between airflows.

In contrast, WSB ash content increased with airflow rates. BC8 exhibited the lowest ash content ( $19.10 \pm 4.17\%$ ), and BC20 had the highest ( $25.06 \pm 3.49\%$ ). The ash content for all airflows presented a correlation of 0.81. As biomass is carbonized, it loses organic material to fuel the reactions; as a result, the inorganic components are relatively increased when quantified with other biochar components.

Table 3 presents the results of the WSB chemical analysis. The primary macronutrients showed contrasting behaviors. For instance, K increased as the temperature and airflow rate rose, from  $4.69 \pm 0.00\%$  (BC8) to  $5.84 \pm 0.10\%$  (BC20), respectively. In contrast, WSB's total N decreased with increasing airflow rate. BC8 presented the highest total N ( $1.26 \pm 0.03\%$ ), and BC20 showed the lowest ( $1.03 \pm 0.04\%$ ). Furthermore, the total N content in BC8 was significantly lower than that from BC12, BC16, and BC20. In addition, total P showed little correlation with the airflow rate ( $R^2 = 0.59$ ). Total P ranged from  $0.45 \pm 0.02\%$  to  $0.48 \pm 0.04\%$  for BC12 and BC20, respectively.

**Table 3.** Airflow effect on wild sugarcane biochar nutrients.

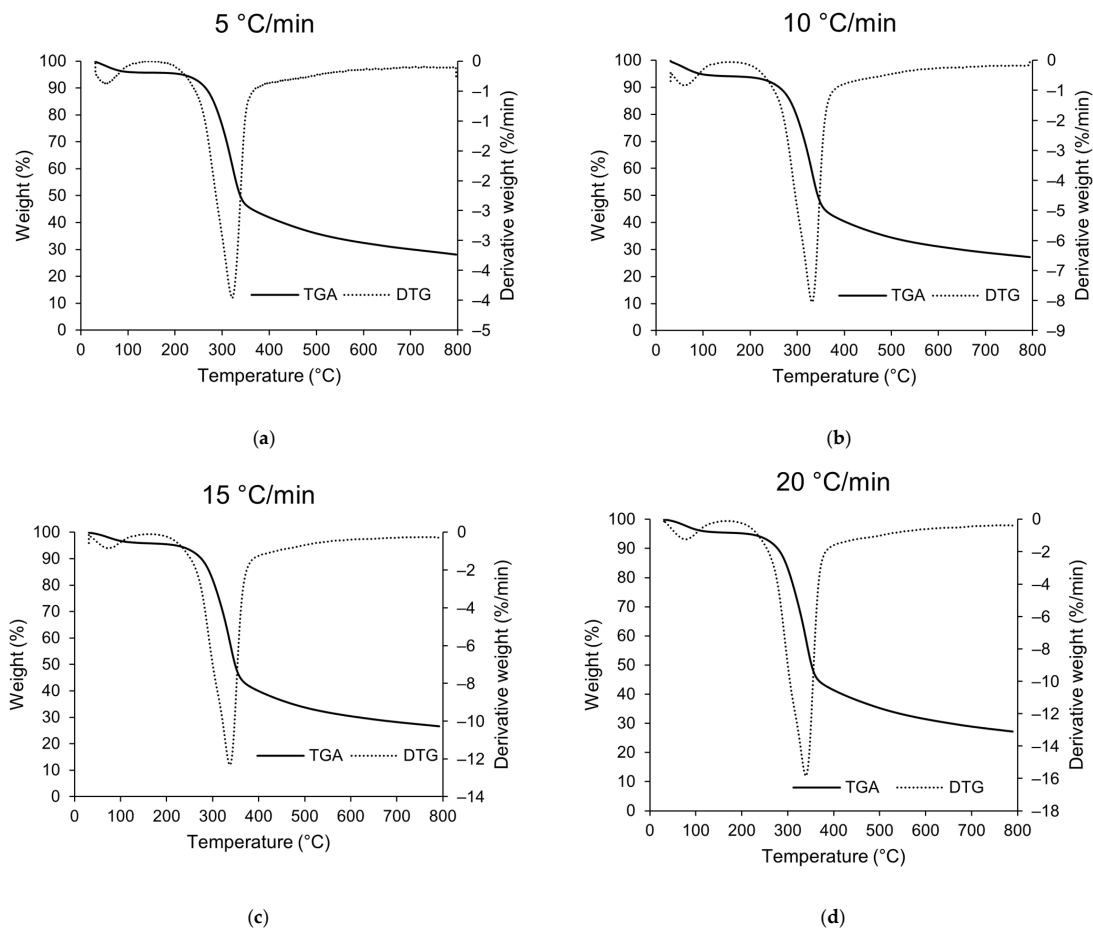
Parameter	Unit	BC8	BC12	BC16	BC20	R <sup>2</sup>
Total N	%	$1.26 \pm 0.03^a$	$1.12 \pm 0.00^b$	$1.10 \pm 0.01^b$	$1.03 \pm 0.04^b$	0.89
Total P	%	$0.46 \pm 0.01^a$	$0.45 \pm 0.02^a$	$0.47 \pm 0.09^a$	$0.48 \pm 0.04^a$	0.59
K	%	$4.69 \pm 0.00^a$	$5.09 \pm 0.07^a$	$5.31 \pm 0.09^b$	$5.84 \pm 0.10^c$	0.97
Mg	%	$0.28 \pm 0.01^{ab}$	$0.26 \pm 0.00^a$	$0.27 \pm 0.02^{ab}$	$0.31 \pm 0.01^b$	0.39
Ca	%	$0.81 \pm 0.08^a$	$0.83 \pm 0.01^a$	$0.86 \pm 0.06^a$	$0.96 \pm 0.01^a$	0.88
Zn	mg/kg	$153.00 \pm 55.15^a$	$167.00 \pm 45.25^a$	$168.50 \pm 50.20^a$	$409.50 \pm 157.68^a$	0.64
O.C.	%	$60.30 \pm 0.23^a$	$61.32 \pm 1.07^a$	$60.42 \pm 1.05^a$	$58.92 \pm 1.09^a$	0.42

O.C.: organic carbon; N: nitrogen; P: phosphorus; K: potassium; Ca: calcium; Zn: zinc. Values followed by a different letter are significantly different at  $\alpha = 0.05$  between airflows.

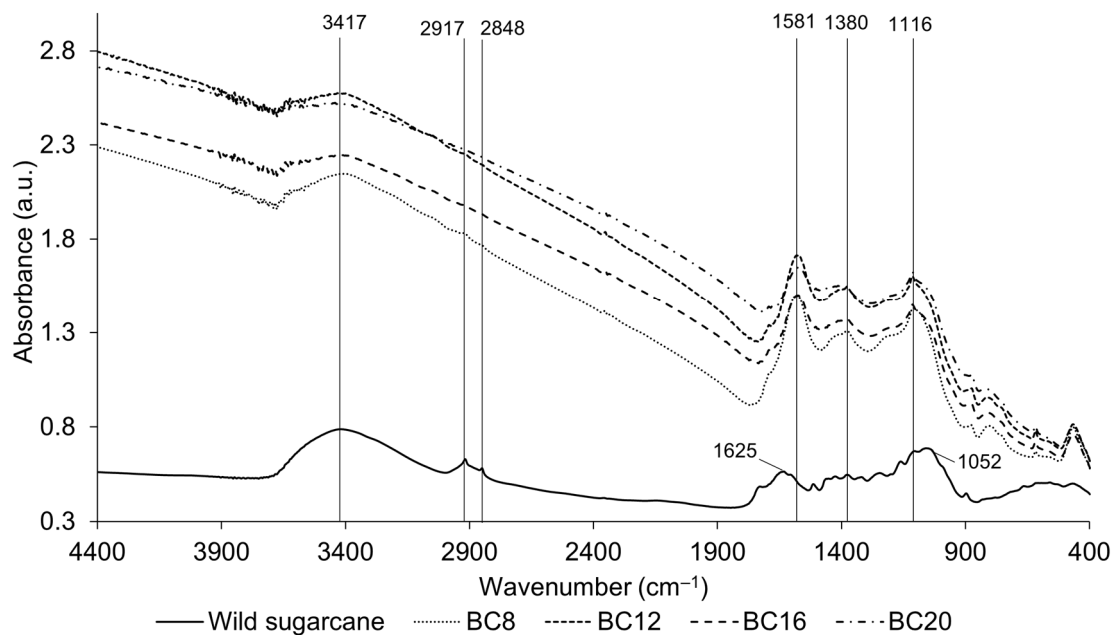
For the secondary nutrients Ca and Mg, the Ca presented an increase ( $R^2 = 0.88$ ) with the airflow rate; however, it did not show a significant difference at various airflows (Table 3). In contrast, Mg did not exhibit a strong linear correlation with airflow rate ( $R^2 = 0.39$ ). However, BC12 and BC20 Mg compositions were found to be significantly different. For the micronutrient Zn, it was observed that its content increased with airflow rates and presented a linear correlation ( $R^2 = 0.64$ ). However, no significant differences were found among the airflow rates. Finally, the organic carbon of wild sugarcane biochar showed little correlation with airflow rate, with  $R^2 = 0.42$ .

Figure 5 shows the results of the wild sugarcane feedstock (WSF) thermogravimetric (TG) and derivative thermogravimetric (DTG) analyses, which were carried out at heating rates of 5, 10, 15, and 20 °C/min. The dehydration, devolatilization, and carbonization stages were observed between 30–195 °C, 195–350 °C, and 350–800 °C. Increasing the heating rate caused the maximum weight loss to increase from 4 to 16%/min.

Figure 6 shows the results of the FTIR analysis of wild sugarcane feedstock and biochar. The feedstock presented peaks at  $3417 \text{ cm}^{-1}$  that correspond to the alcohol/phenolic O-H stretching, which is supposed to be  $3200\text{--}3550 \text{ cm}^{-1}$  [32]. Additionally, the results presented peaks at 2918, 2848, 1625, and 1052 corresponding to asymmetric C-H stretching, symmetric C-H stretching, aromatic C=C carbon stretching, and C-O stretching of alcohol [33–36]. Upon gasification, the absorbance of the O-H stretching at  $3417 \text{ cm}^{-1}$  increased. This could be due to the increase in temperature [32]. Furthermore, peaks at  $1581 \text{ cm}^{-1}$  appeared at all biochars. These peaks correspond to carboxylic acid stretching vibration [37]. The gasification of wild sugarcane also increased the absorbance of aliphatic  $\text{CH}_3$  deformation, which presented at  $1380 \text{ cm}^{-1}$  [36]. P-O stretching peaks appeared after gasification at  $1116 \text{ cm}^{-1}$  [38]. The peaks at 2917 and  $2848 \text{ cm}^{-1}$  disappeared after gasification, which indicates the instability of C- $\text{CH}_3$  links [32].



**Figure 5.** Wild sugarcane biomass thermogravimetric analysis and derivative thermogravimetric at heating rates of: (a) 5 °C/min; (b) 10 °C/min; (c) 15 °C/min; (d) 20 °C/min.



**Figure 6.** Fourier transformed infrared spectroscopy for wild sugarcane and wild sugarcane biochars produced at different airflow rates. BC stands for biochar, and the number represents the airflow rate used for gasification, e.g., BC8—8 L/min.

### 3.2. Atrazine Adsorption

Initial concentrations of 0.5, 1, 3, 5, 10, 15, 20, and 30 mg/L of atrazine were evaluated. The adsorption efficiencies of biochars are shown in Figure 7. All biochar presented a 100% removal efficiency at an initial concentration of 0.5 mg/L. Furthermore, BC12 was the only biochar with 100% removal when the initial concentration was 1 mg/L. At 3 mg/L, BC12 exhibited a higher removal percentage (95.33%), followed by BC16 (69.44%), BC8 (64.44%), and BC20 (61.44%). At 5 mg/L, BC12 (76.73%) and BC16 (75.73%) showed no significant difference in the removal percentage. Meanwhile, BC8 (52.46%) and BC20 (55.60%) showed similar results. An additional increase in atrazine concentration decreased the pollutant removal capacity. At 10 mg/g, BC12 presented the highest removal (68.06%), followed by BC16 (59.73%), BC8 (57.86%), and BC20 (46.80%). A similar pattern was observed when the initial atrazine concentration was increased to 15, 20, and 30 mg/g, where BC12 (60.26, 51.25, and 37.71%) showed the highest removal efficiency, followed by BC8 (48.89, 48.40, and 29.77%) > BC16 (51.00, 33.48, and 25.16%) > BC20 (35.86, 28.45, and 18.73%), respectively.

The atrazine adsorption isotherms are shown in Figure 8, while Table 4 shows the isotherm parameters. The maximum atrazine adsorption capacities were BC8 (0.41 mg/g), BC12 (0.42 mg/g), BC16 (0.28 mg/g), and BC20 (0.22 mg/g). BC8 ( $R^2 = 0.94$ ), BC16 ( $R^2 = 0.96$ ), and BC20 ( $R^2 = 0.98$ ) were better described by the Langmuir isotherm, suggesting monolayer adsorption for these biochar samples [15]. The Langmuir isotherm had a close approximation for BC12 ( $R^2 = 0.95$ ), but the Freundlich isotherm better described the process ( $R^2 = 0.97$ ). Therefore, BC12 might present multilayer, heterogeneous adsorption. The values of  $K_F$  followed the highest (BC12) and lowest (BC20) adsorption capacity. This behavior coincides with the amount of organic and fixed carbon in both biochars, hinting that WSB organic carbon might play a crucial role in organic compounds' sorption [39].

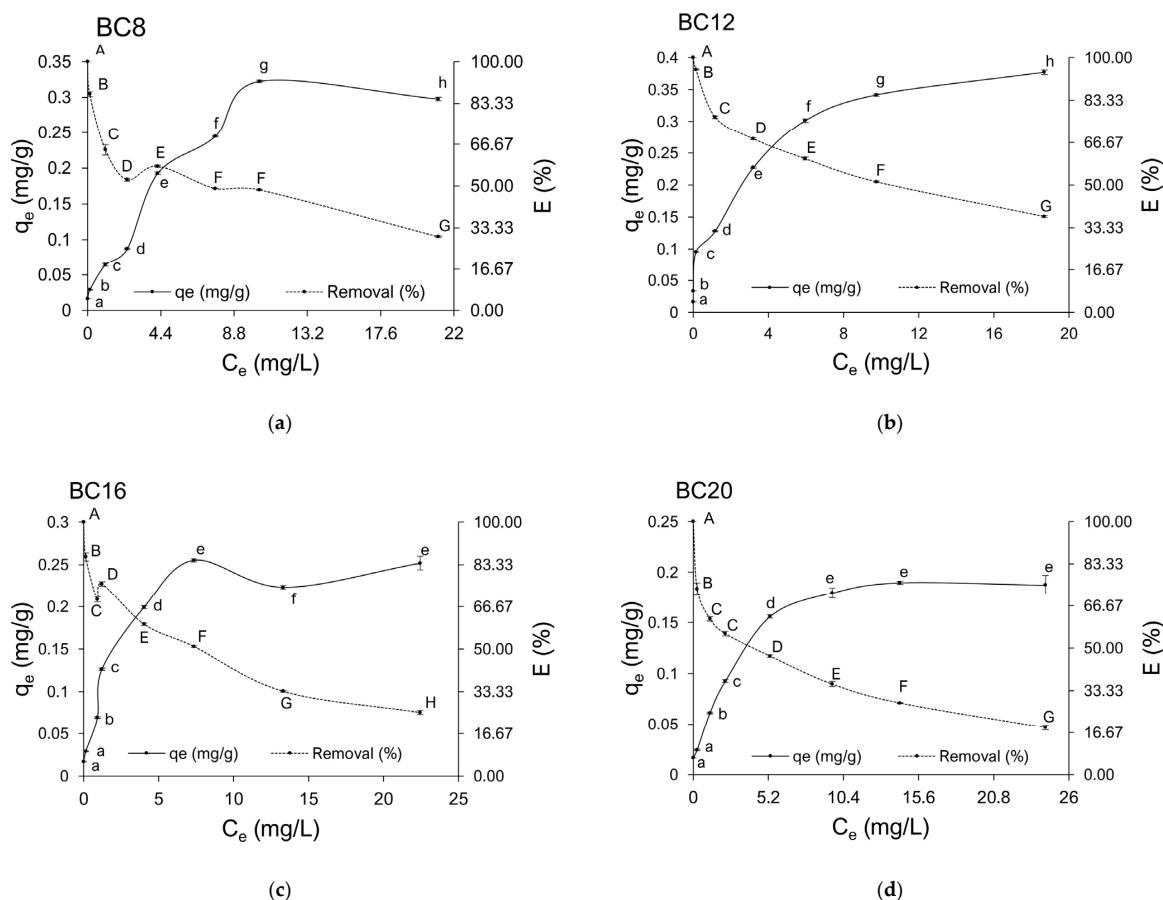


**Figure 7.** Removal efficiency (E) and experimental  $q_e$  for: (a) BC8; (b) BC12; (c) BC16; (d) BC20. Uppercase and lowercase letters indicate significant differences among E and  $q_e$ , respectively.

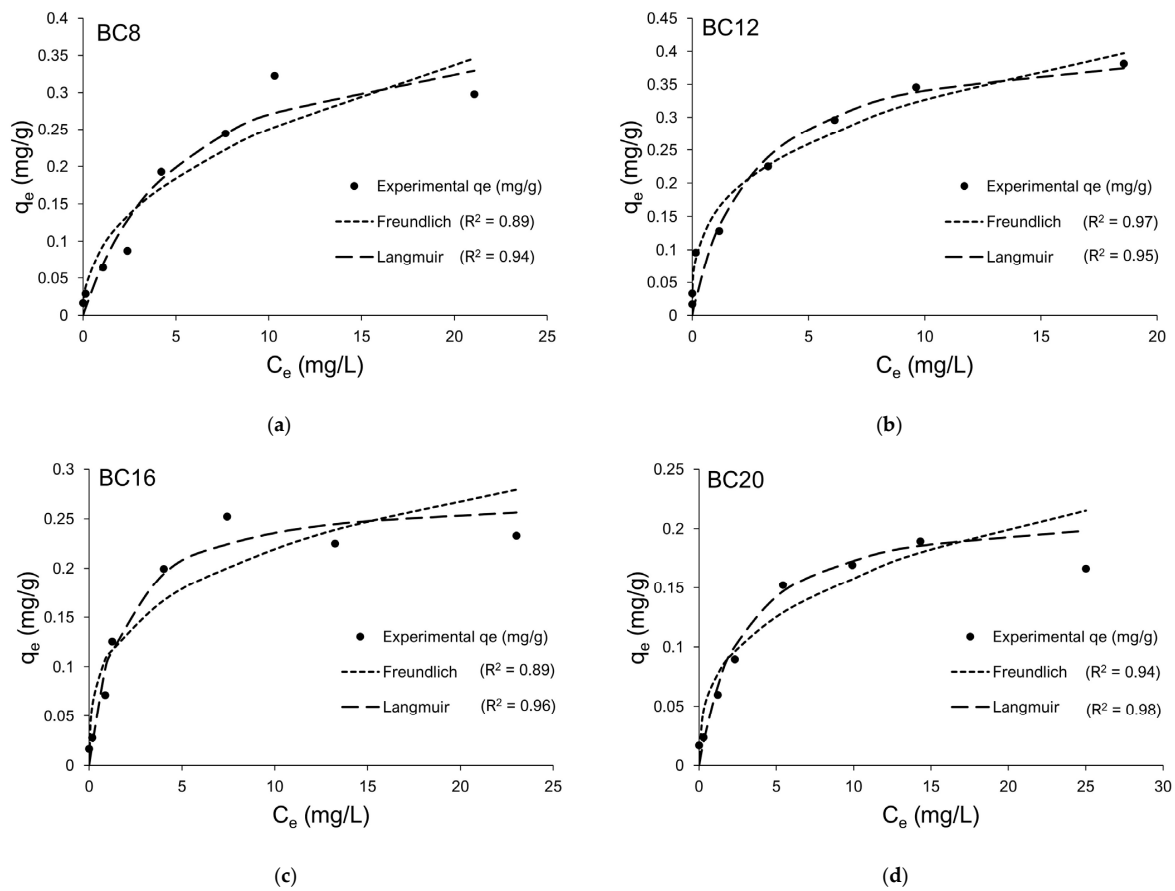


Figure 8. Langmuir and Freundlich isotherms for: (a) BC8; (b) BC12; (c) BC16; (d) BC20.

Table 4. Langmuir and Freundlich isotherm parameters.

Model	Parameter	BC8	BC12	BC16	BC20
Langmuir	$K_L$ (L/mg)	0.19	0.40	0.59	0.38
	$q_m$ (mg/g)	0.41	0.42	0.28	0.22
	$R^2$	0.94	0.95	0.96	0.94
Freundlich	$1/n$	0.43	0.31	0.29	0.33
	$K_F$	0.09	0.16	0.11	0.07
	$((\text{mg/g})(\text{L/mg})^{(1/n)})$				
	$R^2$	0.89	0.97	0.89	0.94

$K_L$ : Langmuir constant;  $q_m$ : maximum adsorption capacity;  $K_F$ : Freundlich constant.

#### 4. Discussion

##### 4.1. Airflow Effect on Biochar Properties

The increase in maximum temperatures reported in this study was similar to the tendency reported by James et al., as they increased the gasification airflow rate and observed a rise in temperature for rice hulls and wood chips biochar [27]. Additionally, Díez et al. reported a similar decrease in yield as airflow rates increased, ranging from 11% to 8% [40]. The reduction in WSB yield can be attributed to the volatilization of material during the carbonization process due to the flaming pyrolysis process in the top-lit updraft gasification. In addition, the increase in temperature promotes the gasification mechanisms leading to higher tar, syngas, and bio-oil production while aiding in volatile matter loss from the biomass [41,42]. Furthermore, the burning rate increase was consistent with the rise in maximum temperature since more biomass material was carbonized at higher temperatures [27].

Wild sugarcane biochar presented a high alkalinity, indicative of the high temperatures achieved and oxidation due to the gasification process. An increase in biochar pH was observed in the James et al. study. Pine wood chips biochar presented an increase in pH as the airflow rate rose due to higher peak reaction temperatures [31]. Furthermore, a pH above nine (9) could indicate an increase in the biochar's aromatic structure and the surface functional groups' representation [43]. The rise in BET surface area is consistent with the volatilization of material during gasification, which promotes a more porous material. Díez et al. found that increasing the airflow rate caused an increase in surface area from 258 to 431 m<sup>2</sup>/g. However, WSB presented a low surface area compared to other biochars used in atrazine removal. Biochar produced from bamboo culm had a BET surface area between 2.72 and 9.21 m<sup>2</sup>/g. Atrazine removal was higher in bamboo culm biochar than in wild sugarcane biochar, with the  $q_m$  being 2.7 and 0.42 mg/g, respectively [43]. WSB's low surface area could suggest strong chemical adsorption instead of physical adsorption. It was observed that the WSB with the highest surface area had the lowest atrazine adsorption, similar to the Mandal et al. study [44].

The fixed carbon and volatile matter showed no linear relation with airflow, which could be explained by the slight difference in the maximum temperatures achieved during the carbonization process. The lack of a linear relationship suggests that WSB's fixed carbon and volatiles peaked at 550 °C. Moreover, the TGA analysis (Figure 5) suggests devolatilization between 330 and 350 °C with little change in the DTG after these temperatures. Furthermore, biomass carbon-based components react at higher temperatures, generating gases transported during the gaseous carbonization phase. Therefore, the reported ash content in WSB may be a relatively fixed amount from the feedstock (5.32%) that appeared to increase with a reduction in carbon content [23].

The volatilization of nitrogen in gaseous forms might be the reason for this behavior, due to its interaction with oxygen at high temperatures, escaping in non-condensable gas in the form of HCN or NH<sub>3</sub> [45,46]. However, phosphorus tends to increase when the temperature rises. The contradictory behavior may be due to the lack of significant temperature differences during WSB production [47]. As Ca did not present a significant difference among airflow rates, it may indicate a fixed quantity in wild sugarcane [48]. WSB had a higher Zn content than corn residue biochar (35.9–71.2 mg/kg), suggesting a good potential for wild sugarcane biochar to improve soil nutrient availability [49].

#### 4.2. Atrazine Adsorption

As seen in Figures 7 and 8, wild sugarcane biochar could be employed to remove atrazine from aqueous solutions. WSB exhibited a higher removal efficiency (46.80–68.06%) of atrazine than soybean straw biochar (10%) at 10 mg/L [50]. In addition, WSB had higher removal efficiency than activated biochar at low concentrations. For example, at 5 mg/L, WSB removed between 52.46 and 76.73% of atrazine, while the activated carbon removed between 19 and 22% of atrazine [22]. Wild sugarcane biochar also had higher atrazine removal capacities (68.06–100%) than bamboo chips, corn cob, eucalyptus bark, rice husk, and rice straw biochars (12.3–70.7%) at initial concentrations ranging from 1 to 10 mg/L [44].

Although WSB presented atrazine removal efficiency between 18.73 and 100%, the atrazine concentration removed was lower than that reported for other biochars. For example, Mandal et al. produced biochar from rice husks and straw that presented  $q_e$  of 0.41 and 0.81 mg/g, respectively [44]. WSB had a removal between 0.15 and 0.25 mg/g at similar conditions. Additionally, WSB had lower  $q_m$  (0.42 mg/g) than *Moringa oleifera* seed husks (4.29 mg/g), *Cedrella fissilis* biochar (6.64 mg/g), and bamboo culm (2.68 mg/g) [13,43,51]. However, wild sugarcane biochar could be modified to improve its adsorption capacity. Wang et al. modified corn stalk biochar with a layered double hydroxide to improve the removal capacity from 95.93 to 143.15 mg/g [52]. Cao et al. prepared nano-MgO-modified fallen leaf biochar, which exhibited 1.99–5.71 times higher atrazine removal capacities than unmodified biochar [15].

Atrazine adsorption was affected by changing the gasification rates. It was observed that the highest adsorption occurred at 12 L/min, which was in accordance with the FTIR analysis and the carbon content (organic and fixed). BC12 presented the highest absorbance at 3417, 1581, 1380, and 1116  $\text{cm}^{-1}$ . The O-H and C-H groups present in the WSB surface could interact with atrazine molecules to improve adsorption [43]. However, further increasing the airflow rate to 16 and 20 L/min decreased the adsorption capacity of WSB. This reduction might be attributed to their lower carbon (fixed and organic) compared with BC12, as seen in Tables 2 and 3.

A suggested mechanism of atrazine adsorption is the formation of H-bonds due to the aromatic compounds in WSB (1581  $\text{cm}^{-1}$ ) [53]. These bands could also represent carboxylic acid, which favorably influences atrazine adsorption [21].  $\pi$ - $\pi$  bonds could also be formed from the aromatic rings of WSB, as previously presented in the literature [33]. Furthermore, the bands of C-O stretch in ether, esters and aromatic alcohols (1112–1114  $\text{cm}^{-1}$ ) could interact with the atrazine molecule with hydrogen bonds. This could make H-bonds or  $\pi$ - $\pi$  bonds the primary mechanisms of WSB for atrazine adsorption [43].

## 5. Conclusions

This study demonstrated that the biomass of *Saccharum spontaneum* L., an invasive species waste, can produce biochar for atrazine removal in aqueous solutions. The biochar was made using a top-lit updraft gasifier with four different airflow rates (8, 12, 16, and 20 L/min). Increasing the airflow rate caused the maximum temperature to increase and the biochar yield to decrease. Despite the low BET surface area of WSC biochar, it achieved removal efficiencies ranging from 18 to 100% for all tested biochar. The removal capacity of wild sugarcane biochar is believed to be associated with the biochar's carboxylic functional groups that promoted atrazine removal. In the same way, the organic carbon composition of the biochar can influence the atrazine removal capacity of wild sugarcane biochar.

The variation in the gasification airflow rate also caused the adsorption capacity to vary. BC8 presented acceptable removal efficiency (29–100%), and it improved with an airflow rate of 12 L/min (37–100%), with the best performance among all wild sugarcane biochars. However, a further increase in the airflow rate caused a decrease in adsorption capacity and efficiency. This reduction in performance was attributed to the decrease in carbon (fixed and organic) content as the airflow rate increased. Therefore, wild sugarcane biochar can be effectively implemented as a potential material for atrazine removal in aqueous media.

**Author Contributions:** Conceptualization, A.M.J.R. and Z.K.; methodology, J.P., A.M.J.R., Z.K. and J.C.; investigation, J.P. and J.C.; data curation, J.P. and A.M.J.R.; writing—original draft preparation J.P.; writing—review and editing, J.P., A.M.J.R. and Z.K.; funding acquisition, A.M.J.R. All authors have read and agreed to the published version of the manuscript.

**Funding:** This research was funded by the Secretaría Nacional de Ciencias, Tecnología e Innovación (SENACYT), grant number 66-2019-ITE18-R2-016, Project title: Carbonización de Biomasa: Aprovechamiento de Residuos Agrícolas para el Mejoramiento de las Propiedades Físico-químicas del Suelo en Áreas de Cultivo—In Spanish, and Sistema Nacional de Investigación (SNI) from the Republic of Panama.

**Data Availability Statement:** Not applicable.

**Acknowledgments:** We thank Ana Sánchez for helping during the biochar production experiments. We also thank Duarte Magalhães, Feyza Kazanc, and the Middle East Technical University Central Lab for the thermogravimetric analysis data. Finally, the authors thank SENACYT for their economic support through the Master of Science programs in Mechanical Engineering and Hydric Resources at the Universidad Tecnológica de Panamá.

**Conflicts of Interest:** The authors declare no conflict of interest.

## References

1. Weidlich, E.W.A.; Flórido, F.G.; Sorrini, T.B.; Brancalion, P.H.S. Controlling Invasive Plant Species in Ecological Restoration: A Global Review. *J. Appl. Ecol.* **2020**, *57*, 1806–1817. [[CrossRef](#)]
2. Saltonstall, K.; Bonnett, G.D. Fire Promotes Growth and Reproduction of *Saccharum spontaneum* (L.) in Panama. *Biol. Invasions* **2012**, *14*, 2479–2488. [[CrossRef](#)]
3. Saltonstall, K.; Bonnett, G.D.; Aitken, K.S. A Perfect Storm: Ploidy and Preadaptation Facilitate *Saccharum Spontaneum* Escape and Invasion in the Republic of Panama. *Biol. Invasions* **2021**, *23*, 1101–1115. [[CrossRef](#)]
4. Gaffar, S.; Dattamudi, S.; Baboukani, A.R.; Chanda, S.; Novak, J.M.; Watts, D.W.; Wang, C.; Jayachandran, K. Physiochemical Characterization of Biochars from Six Feedstocks and Their Effects on the Sorption of Atrazine in an Organic Soil. *Agronomy* **2021**, *11*, 716. [[CrossRef](#)]
5. Hammond, B.W. *Saccharum spontaneum* (Gramineae) in Panama. *J. Sustain. For.* **1998**, *8*, 23–38. [[CrossRef](#)]
6. Maiti, D.; Pandey, V.C. Metal Remediation Potential of Naturally Occurring Plants Growing on Barren Fly Ash Dumps. *Environ. Geochem. Health* **2020**, *43*, 1415–1426. [[CrossRef](#)]
7. Pandey, V.C.; Sahu, N.; Singh, D.P. Physiological Profiling of Invasive Plant Species for Ecological Restoration of Fly Ash Deposits. *Urban Urban Green.* **2020**, *54*, 126773. [[CrossRef](#)]
8. Deago, E.M.; Pizarro, G.E. Denitrification of Drinking Water Using *Saccharum Spontaneum* L. as a Natural Organic Solid Substrate. *J. Water Supply Res. Technol.—AQUA* **2013**, *62*, 477–486. [[CrossRef](#)]
9. Baig, S.A.; Zhu, J.; Muhammad, N.; Sheng, T.; Xu, X. Effect of Synthesis Methods on Magnetic Kans Grass Biochar for Enhanced As(III, V) Adsorption from Aqueous Solutions. *Biomass Bioenergy* **2014**, *71*, 299–310. [[CrossRef](#)]
10. Craven, D.; Hall, J.; Verjan, J.-M. Impacts of Herbicide Application and Mechanical Cleanings on Growth and Mortality of Two Timber Species in *Saccharum Spontaneum* Grasslands of the Panama Canal Watershed. *Restor. Ecol.* **2009**, *17*, 751–761. [[CrossRef](#)]
11. Aguilar, O.; Navarro, D.; Lay, J. Evaluación y Análisis de La Paja Canalera Como Material Biomásico Para La Generación de Energía Eléctrica Mediante Gasificación. *Rev. Iniciación Científica* **2018**, *4*, 14–18. [[CrossRef](#)]
12. Singh, S.; Kumar, V.; Chauhan, A.; Datta, S.; Wani, A.B.; Singh, N.; Singh, J. Toxicity, Degradation and Analysis of the Herbicide Atrazine. *Environ. Chem. Lett.* **2017**, *16*, 211–237. [[CrossRef](#)]
13. Cusioli, L.F.; Bezerra, C.d.O.; Quesada, H.B.; Baptista, A.T.A.; Nishi, L.; Vieira, M.F.; Bergamasco, R. Modified Moringa Oleifera Lam. Seed Husks as Low-Cost Biosorbent for Atrazine Removal. *Environ. Technol.* **2021**, *42*, 1092–1103. [[CrossRef](#)] [[PubMed](#)]
14. Cheng, M.; Zeng, G.; Huang, D.; Lai, C.; Xu, P.; Zhang, C.; Liu, Y.; Wan, J.; Gong, X.; Zhu, Y. Degradation of Atrazine by a Novel Fenton-like Process and Assessment the Influence on the Treated Soil. *J. Hazard. Mater.* **2016**, *312*, 184–191. [[CrossRef](#)] [[PubMed](#)]
15. Cao, Y.; Jiang, S.; Zhang, Y.; Xu, J.; Qiu, L.; Wang, L. Investigation into Adsorption Characteristics and Mechanism of Atrazine on Nano-MgO Modified Fallen Leaf Biochar. *J. Environ. Chem. Eng.* **2021**, *9*, 105727. [[CrossRef](#)]
16. Tao, Y.; Han, S.; Zhang, Q.; Yang, Y.; Shi, H.; Akindolie, M.S.; Jiao, Y.; Qu, J.; Jiang, Z.; Han, W.; et al. Application of Biochar with Functional Microorganisms for Enhanced Atrazine Removal and Phosphorus Utilization. *J. Clean. Prod.* **2020**, *257*, 120535. [[CrossRef](#)]
17. Oladele, S.O. Changes in Physicochemical Properties and Quality Index of an Alfisol after Three Years of Rice Husk Biochar Amendment in Rainfed Rice—Maize Cropping Sequence. *Geoderma* **2019**, *353*, 359–371. [[CrossRef](#)]
18. Yang, X.; Meng, J.; Lan, Y.; Chen, W.; Yang, T.; Yuan, J.; Liu, S.; Han, J. Effects of Maize Stover and Its Biochar on Soil CO<sub>2</sub> Emissions and Labile Organic Carbon Fractions in Northeast China. *Agric. Ecosyst. Environ.* **2017**, *240*, 24–31. [[CrossRef](#)]
19. Hale, S.E.; Nurida, N.L.; Jubaedah; Mulder, J.; Sørmo, E.; Silvani, L.; Abiven, S.; Joseph, S.; Taherymoosavi, S.; Cornelissen, G. The Effect of Biochar, Lime and Ash on Maize Yield in a Long-Term Field Trial in a Ultisol in the Humid Tropics. *Sci. Total Environ.* **2020**, *719*, 137455. [[CrossRef](#)]
20. Qiu, B.; Tao, X.; Wang, H.; Li, W.; Ding, X.; Chu, H. Biochar as a Low-Cost Adsorbent for Aqueous Heavy Metal Removal: A Review. *J. Anal. Appl. Pyrolysis* **2021**, *155*. [[CrossRef](#)]
21. Liu, N.; Charrua, A.B.; Weng, C.H.; Yuan, X.; Ding, F. Characterization of Biochars Derived from Agriculture Wastes and Their Adsorptive Removal of Atrazine from Aqueous Solution: A Comparative Study. *Bioresour. Technol.* **2015**, *198*, 55–62. [[CrossRef](#)] [[PubMed](#)]
22. do Nascimento, C.T.; Vieira, M.G.A.; Scheufele, F.B.; Palú, F.; da Silva, E.A.; Borba, C.E. Adsorption of Atrazine from Aqueous Systems on Chemically Activated Biochar Produced from Corn Straw. *J. Environ. Chem. Eng.* **2022**, *10*, 107039. [[CrossRef](#)]
23. James, A.; Yuan, W.; Boyette, M.; Wang, D.; Kumar, A. Characterization of Biochar from Rice Hulls and Wood Chips Produced in a Top-Lit Updraft Biomass Gasifier. *Trans. ASABE* **2016**, *59*, 749–756. [[CrossRef](#)]
24. Standard Test Method for Moisture in the Analysis Sample of Coal and Coke. Available online: [https://www.astm.org/d3173\\_d3173m-17a.html](https://www.astm.org/d3173_d3173m-17a.html) (accessed on 12 November 2022).
25. Standard Test Method for Volatile Matter in the Analysis Sample of Coal and Coke. Available online: <https://www.astm.org/d3175-89ar97.html> (accessed on 12 November 2022).
26. Standard Practice for Proximate Analysis of Coal and Coke. Available online: <https://www.astm.org/d3172-89r02.html> (accessed on 12 November 2022).

27. James, R.A.M.; Yuan, W.; Boyette, M.D.; Wang, D. Airflow and Insulation Effects on Simultaneous Syngas and Biochar Production in a Top-Lit Updraft Biomass Gasifier. *Renew. Energy* **2018**, *117*, 116–124. [[CrossRef](#)]
28. Standard Methods Committee of the American Public Health Association. American Water Works Association; Water Environment Federation 4500-H+ PH VALUE. In *Standard Methods For the Examination of Water and Wastewater*; Baird, R., Eaton, A., Rice, E., Bridgewater, L., Eds.; American Public Health Association: Washington, DC, USA, 2017.
29. AOAC International. *Official Methods of Analysis of AOAC International*, 18th ed.; Horwitz, W., Latimer, G., Eds.; AOAC International: Gaithersburg, MD, USA, 2005.
30. Bethancourt, G.; James, A.; Villarreal, J.E.; Marín-Calvo, N. Biomass Carbonization-Production and Characterization of Biochar from Rice Husks. In Proceedings of the 2019 7th International Engineering, Sciences and Technology Conference (IESTEC), Panama City, Panama, 9–11 October 2019.
31. James, R.A.M.; Yuan, W.; Wang, D.; Wang, D.; Kumar, A. The Effect of Gasification Conditions on the Surface Properties of Biochar Produced in a Top-Lit Updraft Gasifier. *Appl. Sci.* **2020**, *10*, 688. [[CrossRef](#)]
32. Zhao, Y.; Feng, D.; Zhang, Y.; Huang, Y.; Sun, S. Effect of Pyrolysis Temperature on Char Structure and Chemical Speciation of Alkali and Alkaline Earth Metallic Species in Biochar. *Fuel Process. Technol.* **2016**, *141*, 54–60. [[CrossRef](#)]
33. Binh, Q.A.; Nguyen, V.H.; Kajitvichyanukul, P. Influence of Pyrolysis Conditions of Modified Corn Cob Bio-Waste Sorbents on Adsorption Mechanism of Atrazine in Contaminated Water. *Environ. Technol. Innov.* **2022**, *26*, 102381. [[CrossRef](#)]
34. Mujtaba, G.; Hayat, R.; Hussain, Q.; Ahmed, M. Physico-Chemical Characterization of Biochar, Compost and Co-Composted Biochar Derived from Green Waste. *Sustainability* **2021**, *13*, 4628. [[CrossRef](#)]
35. Abbas, Q.; Liu, G.; Yousaf, B.; Ali, M.U.; Ullah, H.; Munir, M.A.M.; Liu, R. Contrasting Effects of Operating Conditions and Biomass Particle Size on Bulk Characteristics and Surface Chemistry of Rice Husk Derived-Biochars. *J. Anal. Appl. Pyrolysis* **2018**, *134*, 281–292. [[CrossRef](#)]
36. Uras, Ü.; Carrier, M.; Hardie, A.G.; Knoetze, J.H. Physico-Chemical Characterization of Biochars from Vacuum Pyrolysis of South African Agricultural Wastes for Application as Soil Amendments. *J. Anal. Appl. Pyrolysis* **2012**, *98*, 207–213. [[CrossRef](#)]
37. Tong, X.J.; Li, J.Y.; Yuan, J.H.; Xu, R.K. Adsorption of Cu(II) by Biochars Generated from Three Crop Straws. *Chem. Eng. J.* **2011**, *172*, 828–834. [[CrossRef](#)]
38. Lee, M.E.; Park, J.H.; Chung, J.W. Adsorption of Pb(II) and Cu(II) by Ginkgo-Leaf-Derived Biochar Produced under Various Carbonization Temperatures and Times. *Int. J. Environ. Res. Public Health* **2017**, *14*, 1528. [[CrossRef](#)] [[PubMed](#)]
39. Wang, P.; Liu, X.; Yu, B.; Wu, X.; Xu, J.; Dong, F.; Zheng, Y. Characterization of Peanut-Shell Biochar and the Mechanisms Underlying Its Sorption for Atrazine and Nicosulfuron in Aqueous Solution. *Sci. Total Environ.* **2020**, *702*, 134767. [[CrossRef](#)] [[PubMed](#)]
40. Díez, H.E.; Pérez, J.F. Effects of Wood Biomass Type and Airflow Rate on Fuel and Soil Amendment Properties of Biochar Produced in a Top-lit Updraft Gasifier. *Environ. Prog. Sustain. Energy* **2019**, *38*, 13105. [[CrossRef](#)]
41. Cui, X.; Shen, Y.; Yang, Q.; Kawi, S.; He, Z.; Yang, X.; Wang, C.-H. Simultaneous Syngas and Biochar Production during Heavy Metal Separation from Cd/Zn Hyperaccumulator (*Sedum alfredii*) by Gasification. *Chem. Eng. J.* **2018**, *347*, 543–551. [[CrossRef](#)]
42. Gai, X.; Wang, H.; Liu, J.; Zhai, L.; Liu, S.; Ren, T.; Liu, H. Effects of Feedstock and Pyrolysis Temperature on Biochar Adsorption of Ammonium and Nitrate. *PLoS ONE* **2014**, *9*, e113888. [[CrossRef](#)] [[PubMed](#)]
43. Sbizzaro, M.; Sampaio, S.C.; dos Reis, R.R.; Beraldi, F.d.A.; Rosa, D.M.; Maia, C.M.B.D.F.; Cordovil, C.S.d.C.M.d.S.; Nascimento, C.T.D.; da Silva, E.A.; Borba, C.E. Effect of Production Temperature in Biochar Properties from Bamboo Culm and Its Influences on Atrazine Adsorption from Aqueous Systems. *J. Mol. Liq.* **2021**, *343*, 117667. [[CrossRef](#)]
44. Mandal, A.; Singh, N.; Purakayastha, T.J. Characterization of Pesticide Sorption Behaviour of Slow Pyrolysis Biochars as Low Cost Adsorbent for Atrazine and Imidacloprid Removal. *Sci. Total Environ.* **2017**, *577*, 376–385. [[CrossRef](#)]
45. Mandal, S.; Donner, E.; Vasileiadis, S.; Skinner, W.; Smith, E.; Lombi, E. The Effect of Biochar Feedstock, Pyrolysis Temperature, and Application Rate on the Reduction of Ammonia Volatilisation from Biochar-Amended Soil. *Sci. Total Environ.* **2018**, *627*, 942–950. [[CrossRef](#)]
46. Xu, S.; Chen, J.; Peng, H.; Leng, S.; Li, H.; Qu, W.; Hu, Y.; Li, H.; Jiang, S.; Zhou, W.; et al. Effect of Biomass Type and Pyrolysis Temperature on Nitrogen in Biochar, and the Comparison with Hydrochar. *Fuel* **2021**, *291*, 120128. [[CrossRef](#)]
47. Kloss, S.; Zehetner, F.; Dellantonio, A.; Hamid, R.; Ottner, F.; Liedtke, V.; Schwanninger, M.; Gerzabek, M.H.; Soja, G. Characterization of Slow Pyrolysis Biochars: Effects of Feedstocks and Pyrolysis Temperature on Biochar Properties. *J. Environ. Qual.* **2012**, *41*, 990–1000. [[CrossRef](#)] [[PubMed](#)]
48. Escalante Rebolledo, A.; Pérez López, G.; Hidalgo Moreno, C.; López Collado, J.; Campo Alves, J.; Valtierra Pacheco, E.; Etchevers Barra, J. Biocarbón (Biochar) I: Naturaleza, Historia, Fabricación y Uso En El Suelo. *Terra Latinoam.* **2016**, *34*, 367–382.
49. Karimi, A.; Moezzi, A.; Chorom, M.; Enayatizamir, N. Application of Biochar Changed the Status of Nutrients and Biological Activity in a Calcareous Soil. *J. Soil Sci. Plant Nutr.* **2019**, *20*, 450–459. [[CrossRef](#)]
50. Zhang, Y.; Jiang, Q.; Jiang, S.; Li, H.; Zhang, R.; Qu, J.; Zhang, S.; Han, W. One-Step Synthesis of Biochar Supported NZVI Composites for Highly Efficient Activating Persulfate to Oxidatively Degrade Atrazine. *Chem. Eng. J.* **2021**, *420*, 129868. [[CrossRef](#)]
51. Hernandez, P.T.; Franco, S.P.; Georgin, J.; Salau, N.P.G.; Dotto, G.L. Investigation of Biochar from *Cedrella Fissilis* Applied to the Adsorption of Atrazine Herbicide from an Aqueous Medium. *J. Environ. Chem. Eng.* **2022**, *10*, 107408. [[CrossRef](#)]

52. Wang, Y.; Kang, J.; Jiang, S.; Li, H.; Ren, Z.; Xu, Q.; Jiang, Q.; Liu, W.; Li, R.; Zhang, Y. A Composite of Ni–Fe–Zn Layered Double Hydroxides/Biochar for Atrazine Removal from Aqueous Solution. *Biochar* **2020**, *2*, 455–464. [[CrossRef](#)]
53. Tan, G.; Sun, W.; Xu, Y.; Wang, H.; Xu, N. Sorption of Mercury (II) and Atrazine by Biochar, Modified Biochars and Biochar Based Activated Carbon in Aqueous Solution. *Bioresour. Technol.* **2016**, *211*, 727–735. [[CrossRef](#)]

**Disclaimer/Publisher’s Note:** The statements, opinions and data contained in all publications are solely those of the individual author(s) and contributor(s) and not of MDPI and/or the editor(s). MDPI and/or the editor(s) disclaim responsibility for any injury to people or property resulting from any ideas, methods, instructions or products referred to in the content.